AFRL-RW-EG-TR-2014-120

Confined Tension and Triaxial Extension Tests on Eglin High-Strength Concrete

Lance Besaw
Applied Research Associates, Inc.
4300 San Mateo Blvd. NE, Suite A-220
Albuquerque, NM 87110

Daniel Chitty
Applied Research Associates, Inc.
4300 San Mateo Blvd. NE, Suite A-220
Albuquerque, NM 87110

OCTOBER 2014

INTERIM REPORT

AIR FORCE RESEARCH LABORATORY
MUNITIONS DIRECTORATE

■ **Air Force Materiel Command** ■ **United States Air Force** ■ **Eglin Air Force Base, FL 32542**

NOTICE AND SIGNATURE PAGE

Using Government drawings, specifications, or other data included in this document for any purpose other than Government procurement does not in any way obligate the U.S. Government. The fact that the Government formulated or supplied the drawings, specifications, or other data does not license the holder or any other person or corporation; or convey any rights or permission to manufacture, use, or sell any patented invention that may relate to them.

Qualified requestors may obtain copies of this report from the Defense Technical Information Center (DTIC) <http://www.dtic.mil/dtic/index.html>.
.

AFRL-RW-EG-TR-120 HAS BEEN REVIEWED AND IS APPROVED FOR PUBLICATION IN ACCORDANCE WITH ASSIGNED DISTRIBUTION STATEMENT.

FOR THE DIRECTOR:

//SIGNED//

DAVID E. LAMBERT
Ordnance Sciences CTC Lead, Ordnance Division

//SIGNED//

BRADLEY E. MARTIN
Program Manager, Damage Mechanisms Branch

//SIGNED//

MATT J. MATYAC
Technical Advisor, Damage Mechanisms Branch

This report is published in the interest of scientific and technical information exchange, and its publication does not constitute the Government's approval or disapproval of its ideas or findings.

REPORT DOCUMENTATION PAGE

Form Approved
OMB No. 0704-0188

PLEASE DO NOT RETURN YOUR FORM TO THE ABOVE ADDRESS.

1. REPORT DATE *(DD-MM-YYYY)*	2. REPORT TYPE	3. DATES COVERED *(From - To)*
17-10-2014	Interim Report	September 2013 - September 2014

4. TITLE AND SUBTITLE

CONFINED TENSION AND TRIAXIAL EXTENSION TESTS ON EGLIN HIGH-STRENGTH CONCRETE

5a. CONTRACT NUMBER

FA8651-12-D-0309, Task 005

5b. GRANT NUMBER

N/A

5c. PROGRAM ELEMENT NUMBER

6. AUTHOR(S)

(1) Lance Besaw, Applied Research Associates, Inc.

(2) Daniel Chitty, Applied Research Associates, Inc.

5d. PROJECT NUMBER

2502

5e. TASK NUMBER

9210

5f. WORK UNIT NUMBER

W0DT

7. PERFORMING ORGANIZATION NAME(S) AND ADDRESS(ES)

Applied Research Associates, Inc., 4300 San Mateo Blvd NE, Suite A-220
Albuquerque, NM 87110

8. PERFORMING ORGANIZATION REPORT NUMBER

AFRL-RW-EG-TR-2014-120

9. SPONSORING/MONITORING AGENCY NAME(S) AND ADDRESS(ES)

Air Force Research Laboratory, Munitions Directorate, AFRL/RWMW, 101 West Eglin Blvd., Eglin AFB, FL 32542

10. SPONSOR/MONITOR'S ACRONYM(S)

AFRL/RWMW

11. SPONSOR/MONITOR'S REPORT NUMBER(S)

Same as block 8

12. DISTRIBUTION/AVAILABILITY STATEMENT

DISTRIBUTION A. Approved for public release: distribution unlimited (96TW-2014-0199).

13. SUPPLEMENTARY NOTES

14. ABSTRACT

The Air Force Research Laboratory (AFRL) has a need to conduct basic research to understand and implement the necessary physics for materials of interest that increase the accuracy of Finite Element (F.E.) material models. All concretes exhibit higher strength in compression than in tension, therefore it is critical to understand the tensile properties of such materials under varying confinements. These physics need to be accurately modeled in constitutive frameworks (i.e., models) within finite element codes to correctly simulate concrete behavior. This report documents well-controlled quasi-static TriaXial Extension (TXE) and Confined Tension (CT) experiments on Eglin high-strength concrete using a new experimental apparatus design by Applied Research Associates, Inc., Randolph, VT. The experiments developed the tensile failure envelope for this particular material for high-pressure loading up to a maximum mean stress and deviatoric stress of 250 MPa and 275 MPa, respectively. It was found that the tensile failure envelope was distinctly different from that of the compression failure envelope.

15. SUBJECT TERMS

High-strength concrete, tensile properties, triaxial extension, confined tension, high-pressure

16. SECURITY CLASSIFICATION OF:			17. LIMITATION OF ABSTRACT	18. NUMBER OF PAGES	19a. NAME OF RESPONSIBLE PERSON
a. REPORT	b. ABSTRACT	c. THIS PAGE			Bradley E. Martin
UNCLAS	UNCLAS	UNCLAS	SAR	37	19b. TELEPHONE NUMBER *(Include area code)* (850)882-6776

Confined Tension and Triaxial Extension Tests on Eglin High-Strength Concrete

August 16, 2014

Prepared for:
Department of the Air Force, Air Force Material Command
Air Force Research Laboratory – Eglin Research Site

Prepared By:

Lance Besaw, PhD
Daniel Chitty

Applied Research Associates, Inc.
4300 San Mateo Blvd NE, Suite A-220
Albuquerque, NM 87110

.

Contents

1. Background

The Air Force Research Laboratory (AFRL) has a need to conduct basic research to understand and implement the necessary physics for materials of interest that increase the accuracy of Finite Element (F.E.) material models. One area of special interest is improving the material models used in AFRL's F.E. codes for concrete materials. All concretes exhibit higher strength in compression than in tension, therefore it is critical to understand the tensile properties of such materials under varying confinements. The inclusion of such physics gives AFRL researchers ability to correctly simulate concrete behavior under various boundary conditions. To this end, several constitutive models have recently been implemented into AFRLs F.E. code but have not been fully calibrated due to the lack of the necessary data. This task addresses that deficiency.

2. Technical Objectives

The technical objective of this task, as identified in the Statement of Work (SOW), was to obtain confined tension/extension data through a series of quasi-static mechanical property tests under varying levels of confinement for a concrete designated Eglin high-strength concrete. This material was developed by the U.S. Air Force, Eglin AFB, FL and the samples for testing were provided by AFRL. The tests were conducted under two different loading paths; confined tension (CT) and triaxial extension (TXE). Both CT and TXE tests define points on the triaxial extension meridian of the failure surface, defined by two equal principal stresses that are greater (more compressive) than the third principal stress. In TXE, the third (minor) principal stress is less than the other two, but still compressive. In CT, the minor principal stress is tensile. Previously, triaxial compression (TXC) testing was performed on the same material by the U.S. Army Engineer Research and Development Center (ERDC), Vicksburg, MS and the results are reported in Reference 1.

3. Technical Approach

ARA's triaxial loading system is located in our Material Properties Laboratory in Randolph, Vermont. This system is capable of conducting high pressure and load tests on concrete and rock materials. Figure 1 presents photographs of the hydraulic press with and without the steel pressure vessel installed. This system has confining pressure capacity of 400 MPa (58,000 psi) and more than 760,000 lbs. (3.38 MN) of overall loading force. The left panel of Figure 1 shows the system with the pressure vessel removed for unconfined compression testing. The right panel is a photograph of the same system with the heavy steel pressure vessel in position for confined testing. The ARA system has the capability to independently control both confining pressure and axial loading based on real-time feedback from either load or deformation sensors on the test specimen. Test parameters for the CT and TXE tests performed under this task were determined based on the results of triaxial compression tests performed on the same concrete by ERDC (Ref. 1).

Figure 1. Hydraulic press under (left) unconfined and (right) confined operation.

3.1. Definition of Terms

All of the tests reported here were performed on cylindrical specimens. The geotechnical sign convention is used for stresses and strains. Compression is positive and tension is negative. The following symbols are defined:

σ_c = confining pressure, acting on the cylindrical surface of the test specimen

σ_a = axial stress, which is applied along the axis of the specimen

$\sigma_\Delta = \sigma_a - \sigma_c$ = stress difference, which is negative in TXE and CT

$\sigma_m = (\sigma_a + 2\sigma_c)/3$ = mean normal stress or simply mean stress

3.2. Triaxial Extension Testing (TXE)

TXE testing is very similar to the well-known triaxial compression test (TXC). The major difference is that in TXE, the stress difference is negative. That is, the net axial stress, σ_a, is smaller than the confining pressure, σ_c.

3.2.1. TXE Apparatus

The TXE tests were performed in a standard triaxial compression cell, as shown in Figure 2, with a special fixture for TXE loading. The system is based on a load frame with a hydraulic cylinder for axial loading of the test specimen. The other key feature of a TXE apparatus is a pressure vessel with an opening in the top through which axial loading is applied to the end of the test

specimen. With this equipment, it is possible to load the test specimen in various ways by independently controlling: 1) the fluid pressure in the vessel, i.e. the confining pressure; and 2) the axial displacement of the piston. To achieve the negative stress difference, we used a special top cap with integral load cell. Its geometry enables the confining pressure to keep it in contact with the bottom of the axial loading piston. Thus, negative stress difference results from moving the piston upward.

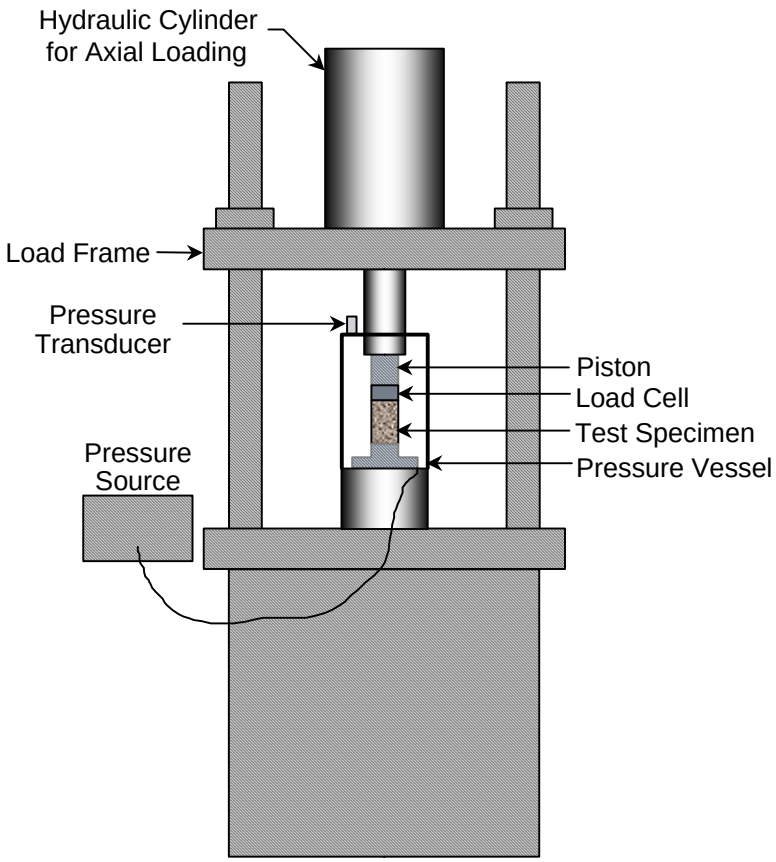

Figure 2. Hydraulic press and pressure vessel diagram showing TXE apparatus.

3.2.2. Specimen Preparation

The concrete specimens were machined to the desired dimensions, 1.875 in diameter by 3.5 in long. When testing with confining pressure, it is important that the specimen be machined to the same diameter as the endcaps so that the jacket is fully supported by a surface that is as smooth and continuous as possible. We used a water-cooled diamond bit to core the specimen. The ends of each specimen were ground flat and parallel to each other, and perpendicular to the cylinder axis (tolerances within 1/1000 inch). Parallelism is particularly important so that the axial stress will be applied as uniformly as possible over the end of the specimen. Visible voids on the cylindrical surface of the specimen were filled with Devcon 5-Minute epoxy.

We encased the specimen in a liquid-tight flexible jacket to exclude the confining fluid from any pore space in the specimen (Figure 3). Typically specimens are jacketed for high-pressure testing

with heat shrinkable 0.02 in polyolefin tubing that is shrunk to the diameter of the specimen and sealed to the steel endcaps with epoxy and wire clamps.

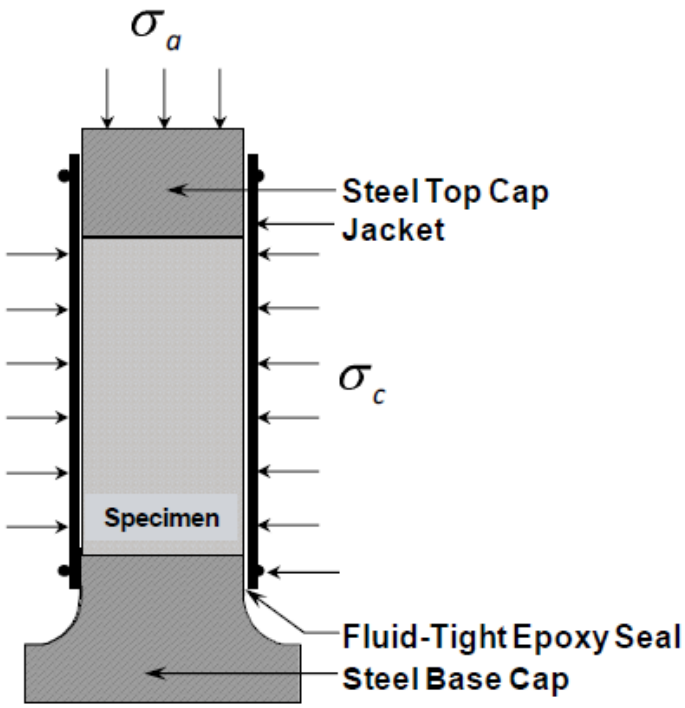

Figure 3. Schematic diagram of test specimen prepared for TXE testing.

TXE tests are especially sensitive to failure of the jacket that separates the specimen from the confining fluid. Since the confining pressure is higher than the axial stress, any amount of confining pressure leakage into the pore space of the specimen will cause the specimen to fracture normal to the specimen axis, resulting in premature conclusion of the test. This is particularly an issue with concrete, which has small air bubbles, some of which are always close enough to the surface so that the confining pressure can push the jacket into the bubble. At higher confining pressures – in excess of about 150 MPa – we wrapped two Kevlar jackets (0.01 in thick) around the specimen prior to installing the polyolefin jacket (0.02 in thick). The Kevlar layers provided the additional support required keeping the jacket from failing, and at the stress levels of these tests, did not significantly affect the results.

3.2.3. Instrumentation

The TXE test was instrumented to measure both loading parameters and specimen response. Confining pressure was measured with a commercial-off-the-shelf (COTS) pressure transducer that is plumbed into the confining pressure system close to the pressure vessel.

In the ARA TXE system, axial loading on the specimen is measured with a load cell inside the pressure vessel. There is significant friction between the piston and the seal in the top of the pressure vessel. With a load cell external to the pressure vessel, it would be virtually impossible to correct for seal friction to find the actual load applied to the specimen. In our high-pressure TXE apparatus, we used a strain-gaged solid steel plug to measure axial loading. The load cells

are constructed using a standard approach in which the strain gages are configured in a full Wheatstone bridge with two axial gages at diametrically opposite locations on the load cell and two circumferential gages, one adjacent to each axial gage. They are wired into the bridge in such a way that the signals from the axial gage add to each other and the signals from the circumferential gages subtract. Since axial loading of the load cell results in compression in the axial direction and expansion in the circumferential direction (due to the Poisson effect), the two negative signs (one due to bridge configuration and one due to Poisson effect) cancel each other and the circumferential gage output actually adds to the signal for a given axial load.

Inside the pressure vessel, the load cell is also subjected to hydrostatic loading by the confining fluid. Under hydrostatic loading, strain in the load cell is equal in all directions and the signals for the axial and circumferential gages cancel each other because of the bridge configuration. An internal load cell constructed in this manner is theoretically insensitive to the hydrostatic load. In practice, there is usually a small sensitivity, which we characterize and eliminate from the data. Figure 4 illustrates a typical instrumentation approach, but not the TXE loading fixture.

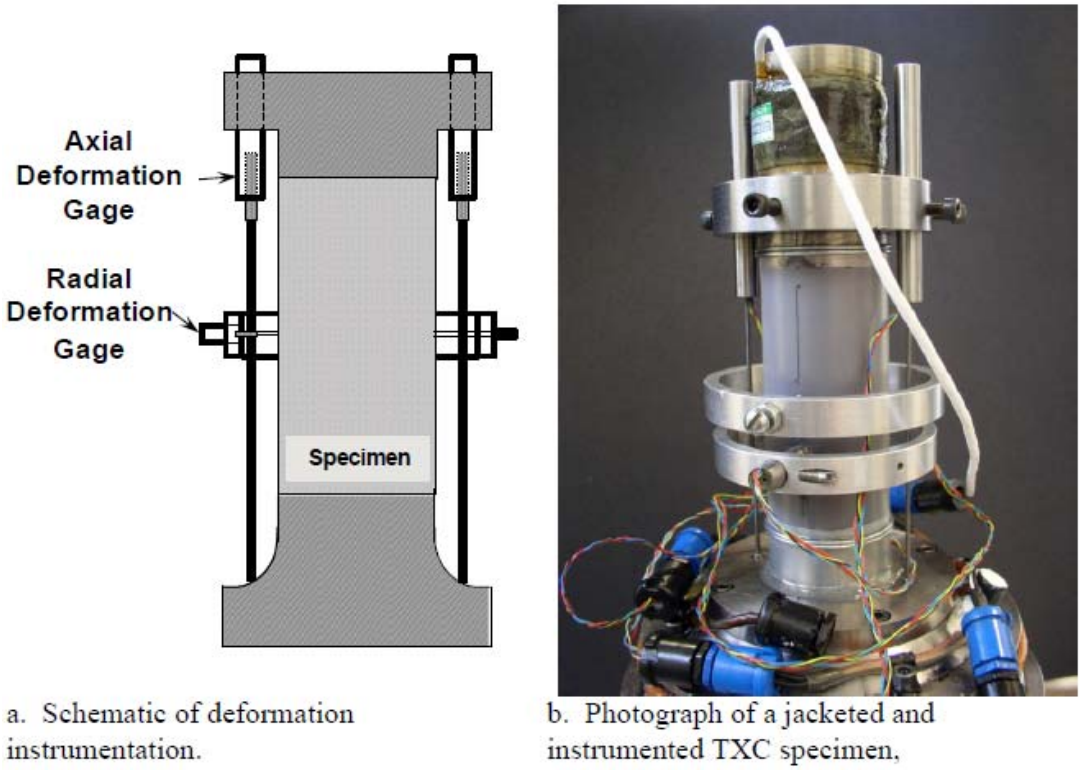

a. Schematic of deformation instrumentation.

b. Photograph of a jacketed and instrumented TXC specimen.

Figure 4. Typical instrumentation of a TXE specimen.

In this work, we used linear variable differential transformers (LVDTs) to measure overall specimen deformation (Figure 4). The body of the LVDT is hollow and contains multiple transformer coils. Moving the core through the bore causes the output current to vary in proportion to the core displacement. As shown in the figure, two diametrically opposite LVDTs were used to sense the axial deformation of the specimen. Because of the way they are attached, they also sense some deformation of the endcaps. The endcap deformation was characterized and eliminated from the records during post-processing. An advantage of axial deformation

measurement with LVDTs attached to the endcaps is that it is possible to achieve good deformation measurements well beyond the point where the specimen begins to break up.

A radial LVDT referenced to a concentric aluminum ring was also installed on each TXE specimen. However the measurements are only indicative of general trends because they include a significant component of compression of the heavy jacket. Further, TXE failures tend to localize at some point along the height of the specimen that is not known *a priori*, and it is unlikely that the radial gage will be positioned correctly to measure the radial deformation at the failure location.

3.3. Confined Tension (CT)

In a CT test, confining pressure loading is applied to the cylindrical surfaces of the specimen and the axial loading can range from hydrostatic (compressive axial stress equal to confining pressure) to tensile, the magnitude of which is limited by the strength of the specimen at the applied confining pressure.

3.3.1. CT Apparatus

The CT testing was performed using a fixture designed by ARA for this purpose, and illustrated in Figure 5. For CT testing, this special-purpose fixture is installed in the standard TXC cell. Because the axial loading in a CT test is tensile, the specimen must be mechanically attached to the loading platens. When the piston of the test machine is advanced, the TXE test fixture mechanically transforms the compressive loading on the fixture into tensile loading on the specimen.

Figure 5. Confined tension apparatus.

3.3.2. Specimen Preparation

Overall the preparation of CT testing specimen was very similar to that of the TXE testing specimen. The concrete specimens were machined to the desired dimensions, 2.0 in diameter by 2.0 in long. Visible voids were filled with Devcon 5-Minute epoxy to support the jacket and prevent leaks. Both the endcaps and the ends of the specimen were sandblasted in preparation for epoxy application. A thin layer of high strength epoxy (Loctite E-20HP) was used to secure the specimen to the endcaps. Loctite E-20HP has an ASTM D638 tensile strength of 40 MPa and tensile elongation of 8%. A specially designed curing fixture (not shown) was used to ensure the specimen and endcaps are concentric, parallel and flat to within 1/1000 in. A heat shrink jacket was installed over the entire specimen to exclude the confining fluid from the pore space of the specimen.

3.3.3. Instrumentation

The instrumentation used for CT testing was similar to those described for TXE testing. Confining pressure was measured with the COTS pressure gage that is part of the standard TXC/TXE suite.

The load cell for stress difference measurement is part of the CT fixture. It is situated so that it directly measures only the load applied to the specimen. Consistent with the TXE load cell, the CT load cell is a solid steel cylinder with strain gages installed in a full bridge configuration.

Strain measurements in the CT tests are challenging, partly because the strains are so small. Concrete loaded in unconfined tension typically fails when axial strain is less than 0.02%. Three LVDTs, 120° apart were used to measure axial deformation of the test specimens. They were attached to shoulders built into the endcaps for that purpose. We used a thin epoxy layer (0.05 inch) between the specimen and endcap to minimize epoxy deformation as compared with specimen deformation. As with the TXE tests, the LVDTs measure some amount of endcap deformation (including epoxy) which was characterized and removed from the records at post-processing. The reported axial strains are based on an average of the three axial deformation measurements. Radial deformation measurements in the CT tests were not made because the CT test fixture is not currently set up to accommodate a radial reference ring.

4. Experimental Results

This Section individually presents the results of the TXE and CT tests. In the following Section TXE and CT strengths are presented together and compared with strengths from the TXE tests presented in Reference 1. The results of both types are summarized in Table 1.

Table 1. Summary of TXE and CT test results.

Test ID	Specimen ID	Test Type	Specimen Length (mm)	Specimen Diameter (mm)	Dry Density Mg/m^3	Ultrasonic Wavespeed Axial (km/s)	Ultrasonic Wavespeed Radial (km/s)	Stress State at Failure Axial (MPa)	Stress State at Failure Radial (MPa)	Stress State at Failure Mean (MPa)	Stress State at Failure Difference (MPa)
M4A14	T19-03	CT: σ_c = 0.0 MPa	53.06	51.10	2.308	4.95	3.95	-4.62	0.00	-1.54	-4.62
M5A/B14	T19-01	CT: σ_c = 22.3 MPa	53.06	51.08	2.306	4.75	4.34	-3.63	22.3	13.66	-25.93
A9A/B14	T19-06	CT: σ_c = 35.0 MPa	53.09	51.08	2.303	4.62	3.64	-2.34	35.0	22.55	-37.34
M6A/B14	T19-02	CT: σ_c = 44.6 MPa	53.09	51.10	2.294	4.78	3.96	-2.18	44.6	29.01	-46.78
A9C/D14	T19-05	CT: σ_c = 65.0 MPa	53.34	51.08	2.269	4.57	4.51	-1.74	65.0	42.75	-66.74
F11B14	T19-10	TXE: σ_m = 80 MPa	95.22	47.19	2.318	4.38	4.71	Did not fail			
A10D14	T19-15	TXE: σ_m = 115 MPa	95.20	47.22	2.316	4.41	4.77	6.68	167.46	113.87	-160.78
F18B14	T19-12	TXE: σ_m = 150 MPa	95.22	47.22	2.327	4.81	4.83	11.16	216.96	148.36	-205.80
A11B14	T19-14	TXE: σ_m = 200 MPa	95.22	47.19	2.309	4.42	4.70	38.63	276.1	196.94	-237.47
F13B14	T19-09	TXE: σ_m = 250 MPa	95.17	47.19	2.316	4.72	4.66	60.12	337.85	245.27	-277.73

4.1. Triaxial Extension (TXE) Test Results

In each TXE test, the initial loading was hydrostatic to a specified level of mean stress. The TXE loading was then applied while holding that mean stress constant. To accomplish this, there was a coordinated increase in confining pressure and decrease in stress difference (and thus in axial stress). This loading scheme is illustrated by Figure 6, which presents the stress paths for the TXE portion of from all five tests in terms of axial stress and confining pressure. The hydrostatic loading is not shown. The shearing, or TXE, portion of each test begins at the solid diamond symbol, which indicates an isotropic stress state at the specified mean stress level. The stress path during TXE loading is down and to the right at a 2:1 slope, which maintains constant mean stress. The open circle symbol on each curve indicates the stress state at failure. The failure stress states are compiled in Table 1. Figure 7 provides an alternate presentation of the stress paths, in terms of mean stress and stress difference.

In test F11A/B14, TXE loading was applied at 80 MPa mean stress. That specimen did not fail. The axial stress decreased to zero without failing the specimen. At that point, the endcaps separate from the specimen and no additional stress difference can be applied. At zero axial stress, the confining pressure was 120 MPa. We only know the material can support that stress state without failure.

Stress-strain curves from the five TXE tests are presented in Figure 8 in terms of axial stress and axial and radial strains. The strains in this figure are incremental from the hydrostatic state. Although not shown on this plot, confining pressure is also changing during the test, as indicated by the stress paths in Figure 6. The TXE strength data are summarized in Table 1. The strength points from all TXE tests are plotted in terms of mean stress and stress difference in Figure 9. Data from individual tests, including pre- and post-test photographs are presented in Appendix A.

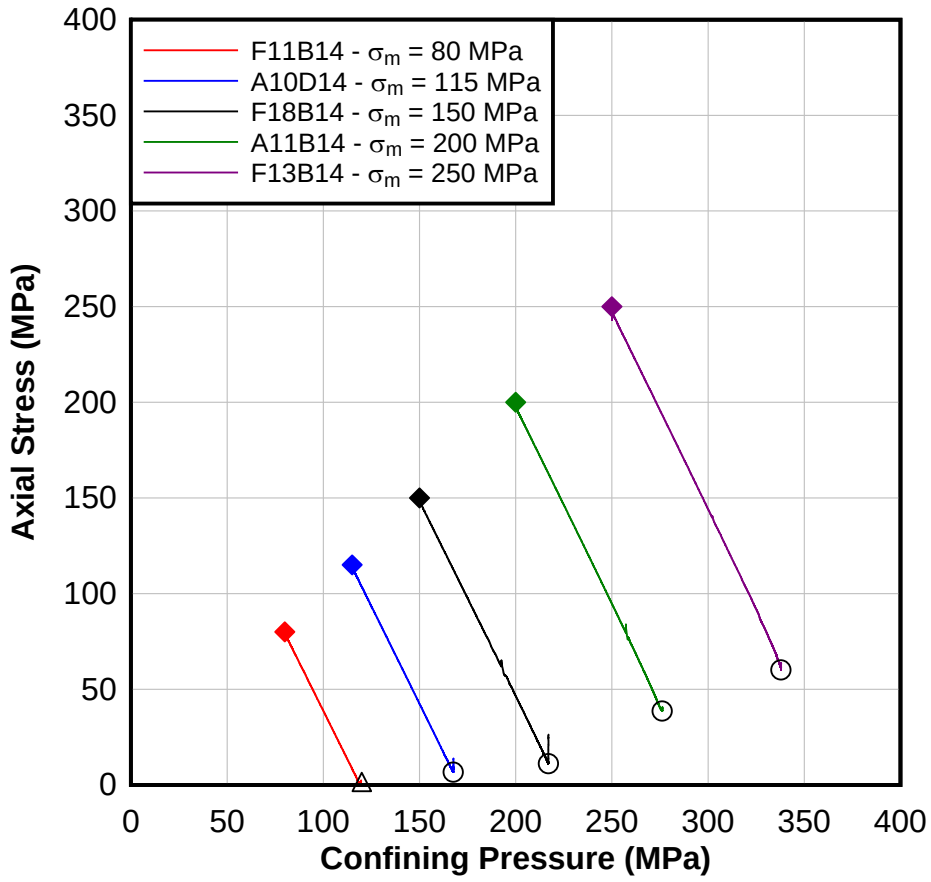

Figure 6. Stress paths of five TXE tests, each at constant mean stress, presented in terms of principal stresses.

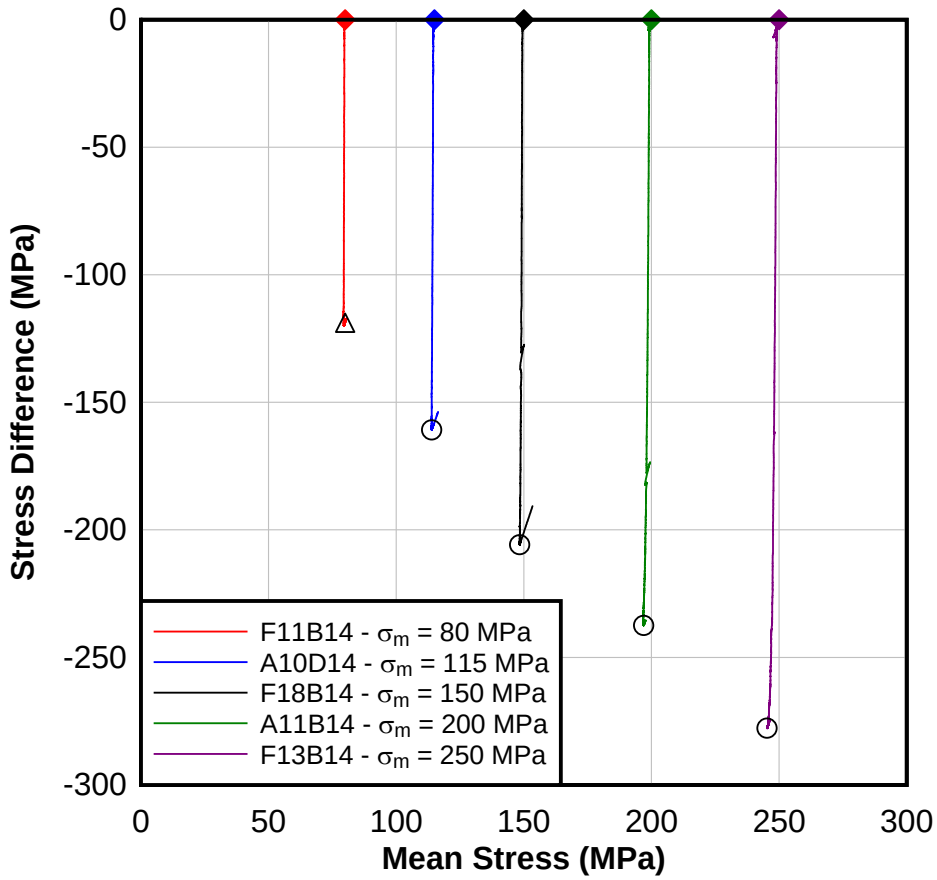

Figure 7. Stress paths of five TXE tests, each at constant mean stress, presented in terms of mean stress and stress difference.

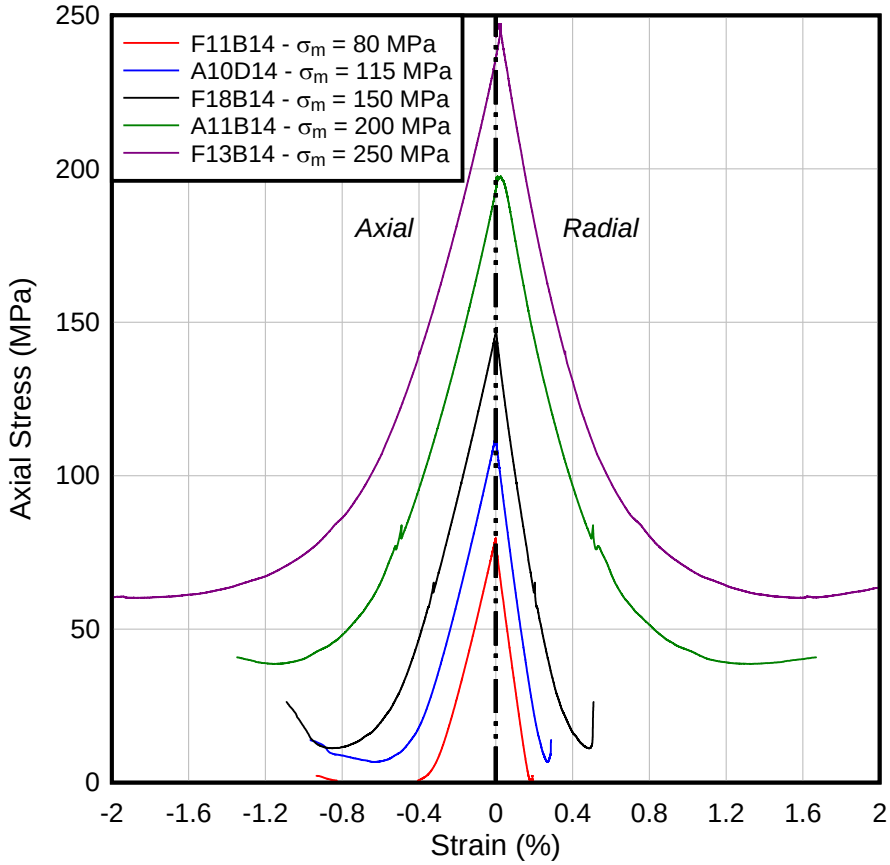

Figure 8. Stress-strain curves from five TXE tests, each at a constant mean stress. Note that the confining pressure is not constant during these tests.

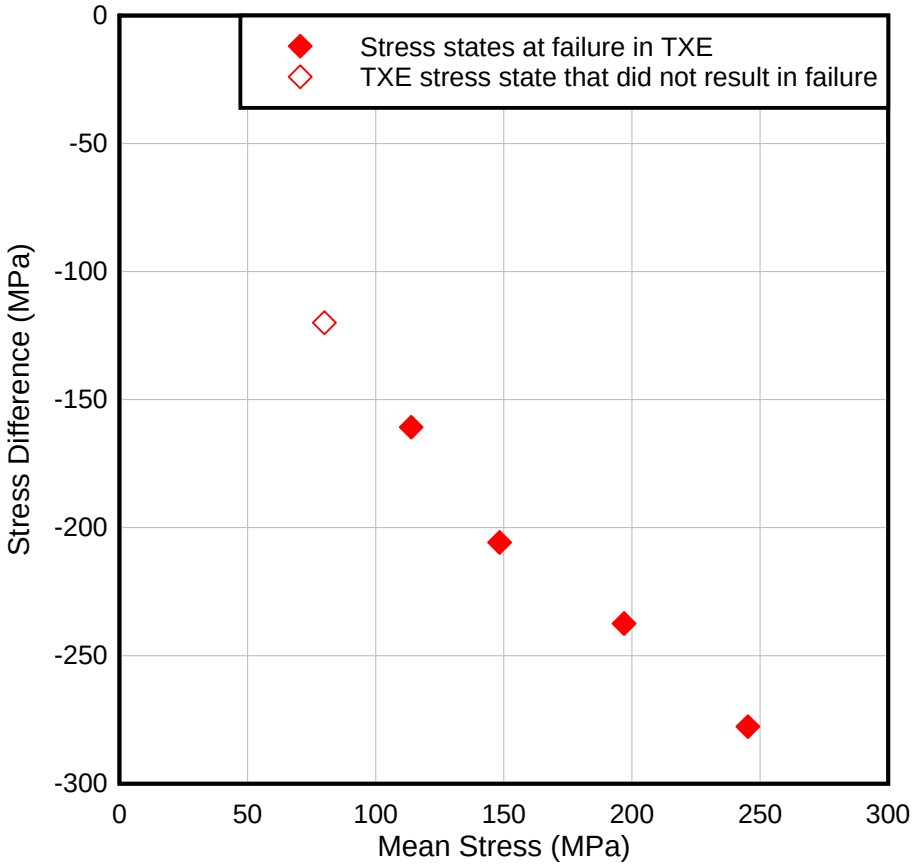

Figure 9. Summary of strength points from TXE tests.

4.2. Confined Tension (CT) Test Results

One of the CT tests was performed with zero confining pressure, i.e. an unconfined tension test. In the confined tests, the initial loading was hydrostatic. Upon reaching a specified hydrostatic stress level, the confining pressure was held constant while negative incremental axial loading was applied to failure using the ARA confined tension apparatus. In order to help maintain control of the tests following tensile failure, stiffening rods were installed in the apparatus in parallel with the specimen in preparation for each test. The force transducer is situated so that it measures only the axial load difference applied to the specimen, not the load in the stiffening elements. Furthermore, the zero baseline readings were taken before installing the stiffening rods so that the axial force and strain measurements are unambiguous. During hydrostatic loading, a small amount of stress difference is applied to the specimen due to dimensional changes in the loading apparatus due to pressurization. These stresses are measured and have no effect on the final outcome of the test.

Stress-strain curves from the five CT tests are presented in Figure 10. The curves in Figure 10 include both the hydrostatic and tensile loading phases of loading. The strains at failure quite

accurately represent the actual axial strains in the specimens. The stress states at failure are compiled in Table 1 and plotted in Figure 11.

Data from individual tests, including pre- and post-test photographs are presented in Appendix B.

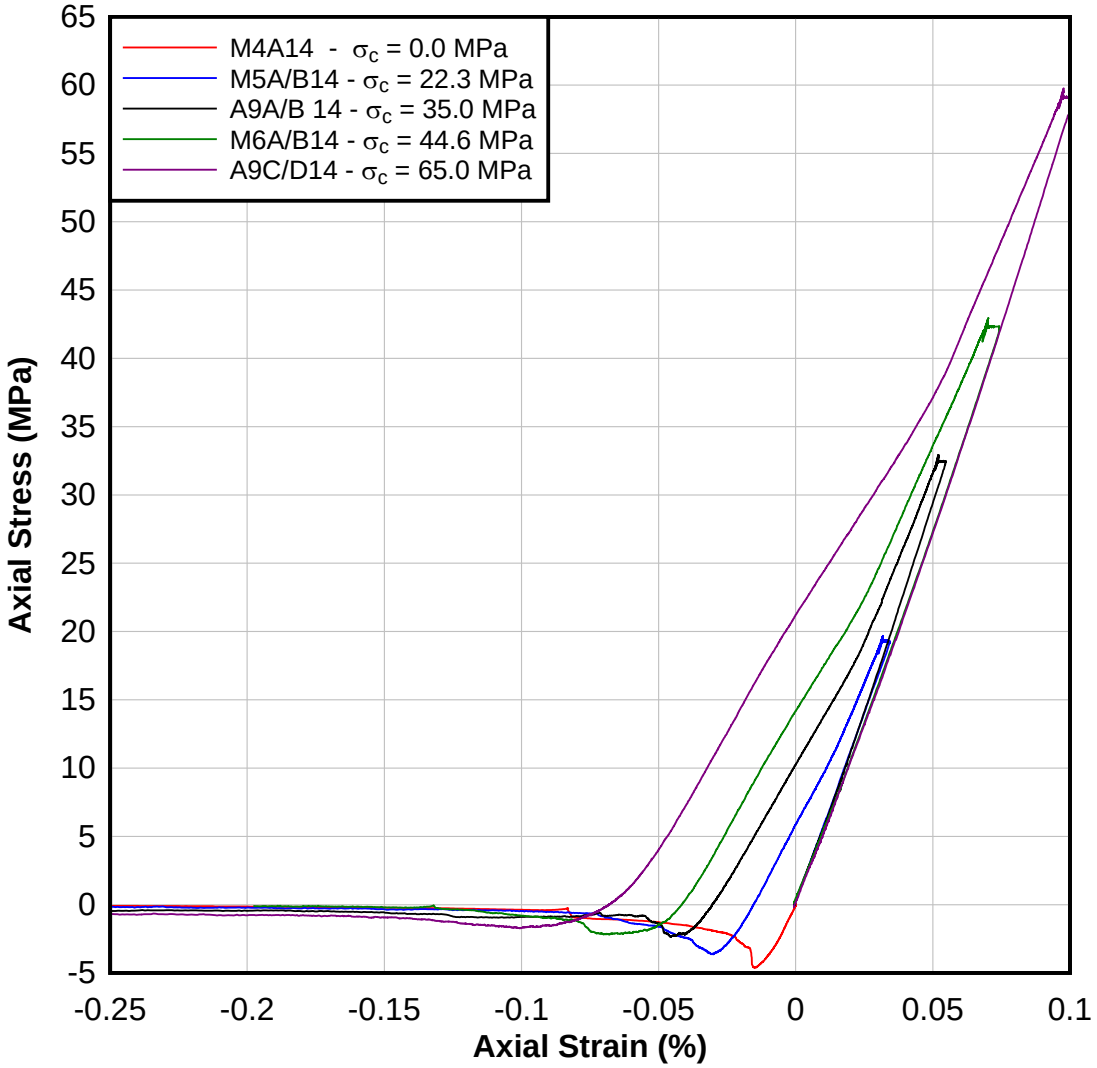

Figure 10. Stress-strain curves from five CT tests, including both hydrostatic and tensile loading phases.

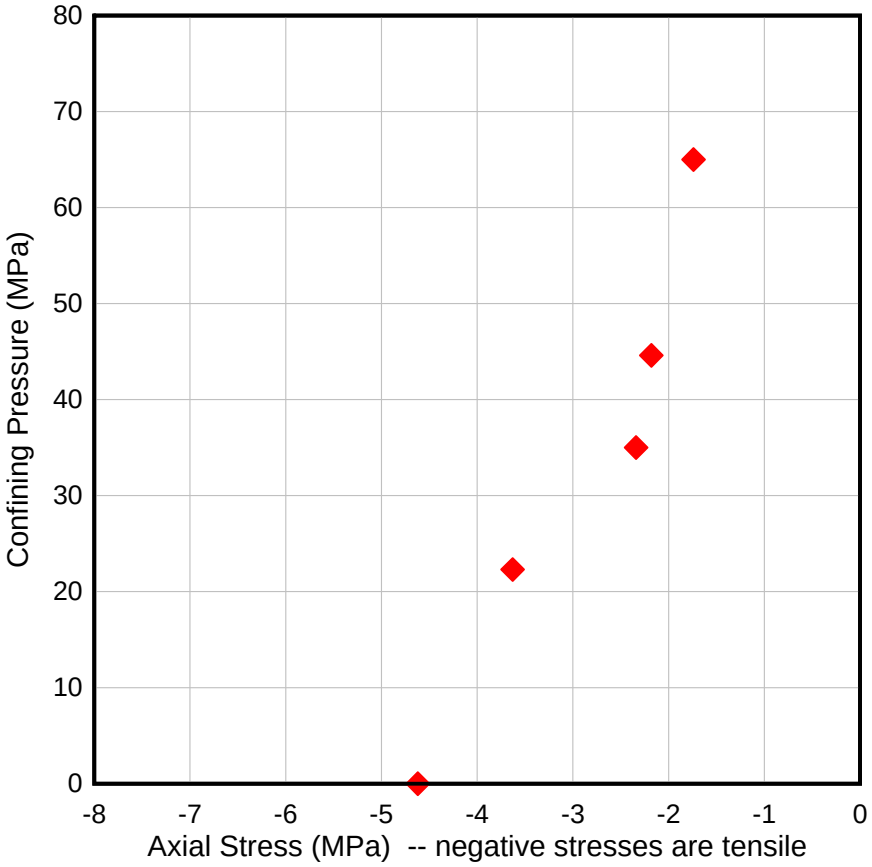

Figure 11. Summary of strength points from CT tests. Note the factor of ten expansion of the horizontal scale relative the vertical.

5. Discussion of Results

The overall objective of performing strength tests on concrete is to define the failure surface of the material, which can be quite complex. Stress states inside the failure surface can be supported by the material, but it will fail (break) if we attempt to apply a state of stress outside the failure surface. The stress state in a material under loading is defined by three principal stresses, which in general can all be different. It is very unusual and requires special equipment to perform tests with three different principal stresses. In conventional TXC tests and in the CT and TXE tests reported herein, there are always two equal principal stresses applied by fluid pressure. In TXC tests, the third principal stress is larger (more compressive) than the other two. In TXE and CT tests, the third principal stress is smaller (less compressive) than the other two (equal) principal stresses. In this Section, the strength points from the tests conducted under this task are summarized in various plots. To put them in context, TXC data from Reference 1 are included where appropriate.

Figure 12 presents the failure stress states from the CT and TXE tests in terms of minimum and maximum principal stresses. Recall that the minimum principal stress is in the axial direction

and the maximum principal stress is applied by fluid pressure in the other two directions. Also show in Figure 12, are strength points from the ERDC TXC tests. For those points, the maximum principal stress is in the axial direction and the minimum principal stress is applied by hydraulic fluid in the other two directions. Figure 12 also presents a bilinear fit that reasonably represents the combined dataset, keeping in mind that we do not know how nearly identical the material tested by ERDC is to the concrete tested in the ARA laboratory. Representing strength points on the TXE and TXC meridians with the same curve is consistent with the assumption that strength is independent of intermediate principal stress – or the Mohr-Coulomb assumption.

Constitutive models in numerical simulation programs are not typically formulated in terms of minimum and maximum principal stresses. It is far more common to have plasticity models formulated in terms of some other stress invariants such as mean stress and the square root of the second invariant of the stress deviator tensor. For TXC and TXE (including CT) stress states, which have two equal principal stresses, the absolute value of stress difference is equal to the square root of (three time the second invariant of the stress deviator tensor). The TXE and CT strength points are presented in terms of mean stress and stress difference in Figure 13. This is a natural set of coordinates from a laboratory testing perspective. In Figure 14, the same data are presented, along with the ERDC TXC data in terms of mean stress and absolute value of stress difference. Here, the TXC and TXE data clearly form different curves, corresponding to the different meridians of the failure surface. The fit lines on Figure 13 and Figure 14 represent the same stress states as the line on Figure 12, transformed into the appropriate coordinates.

We believe the slope break in the fit lines corresponds, at least approximately, to the transition between extension to shear modes of failure, which is probably more gradual in TXC than in TXE.

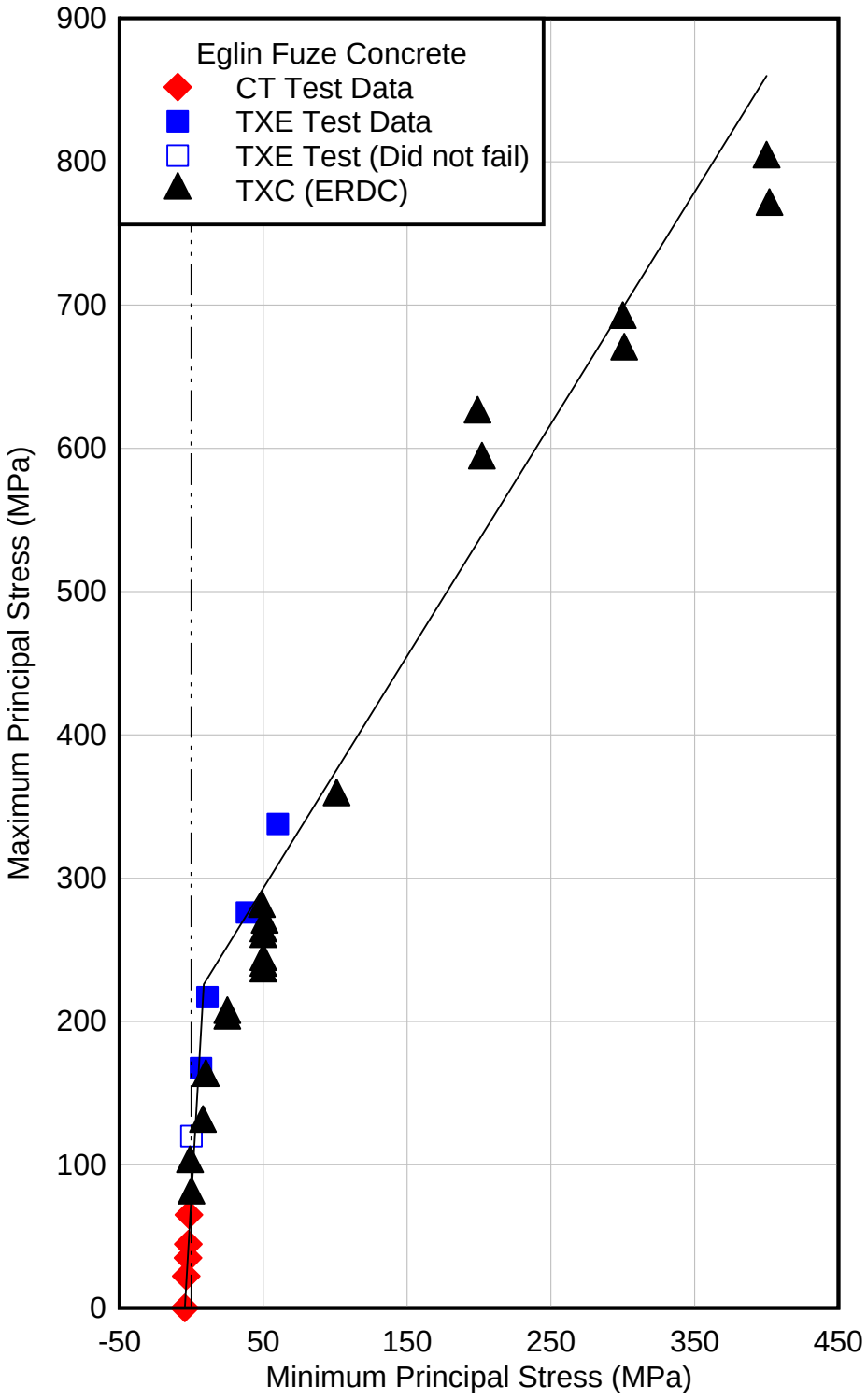

Figure 12. Strength points from TXE and CT tests plotted along with TXC data from Reference 1 in terms of minimum and maximum principal stresses.

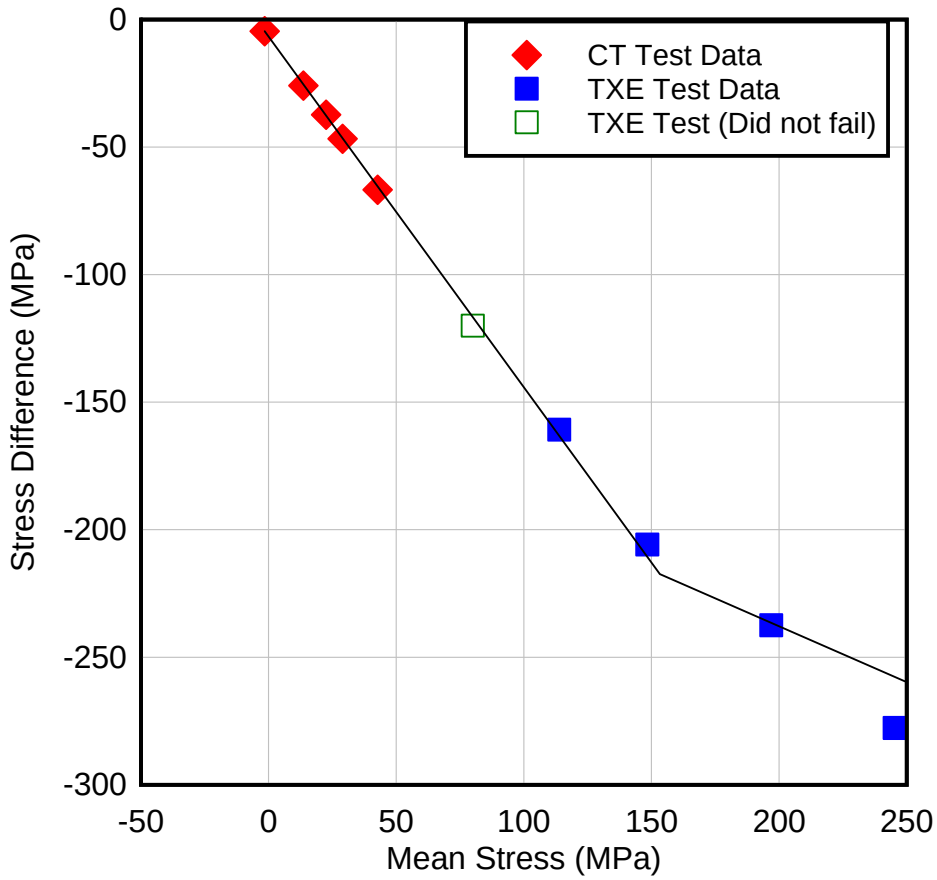

Figure 13. TXE and CT strengths plotted in terms of mean stress and stress difference.

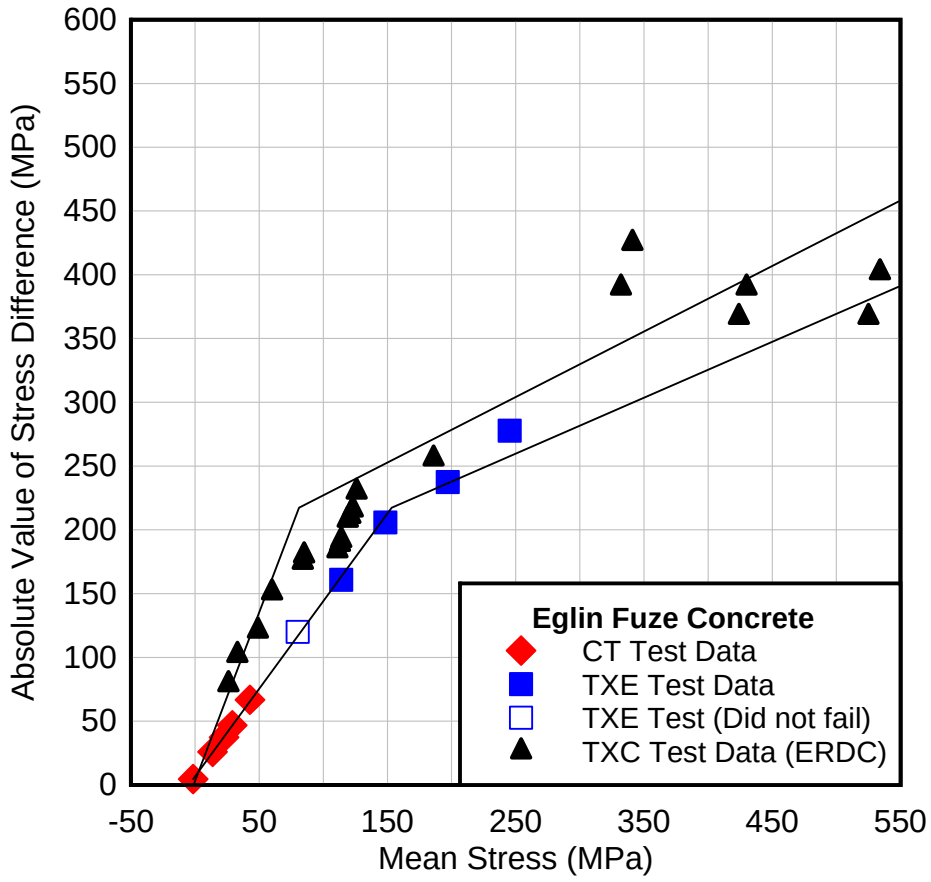

Figure 14. Strength points from TXE and CT tests plotted along with TXC data from Reference 1 in terms of mean stress and the absolute value of stress difference.

6. References

1. Williams, E. S. (2008). *Laboratory Characterization of Eglin Fuze and Holloman Fuze Concretes.* Vicksburg, MS: ERDC/GSL TR-08-12.

7. Appendix A – Triaxial Extension (TXE) Data and Photos

Test F11A/B14 – Triaxial Extension at 80 MPa Mean Stress

DID NOT FAIL

Pre-test

Post-test

F11B14

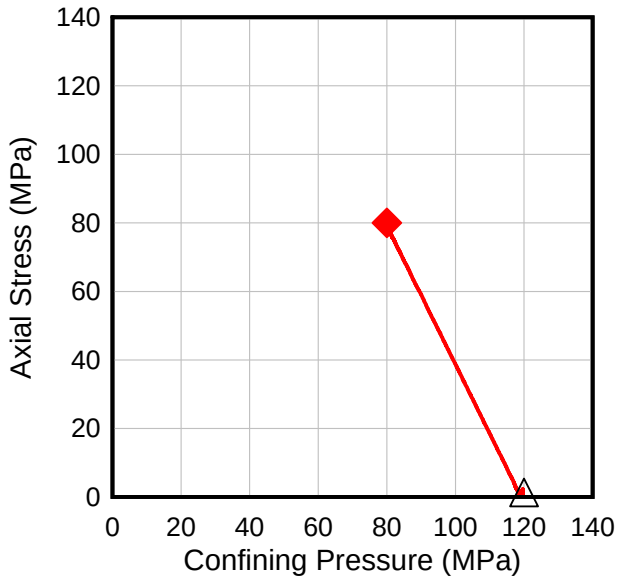

F11B14

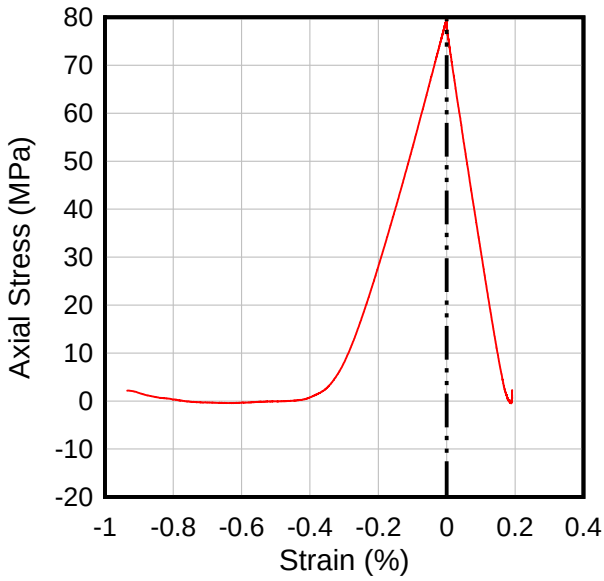

Test A10C/D14 – Triaxial Extension at 115 MPa Mean Stress

Pre-test

Post-test

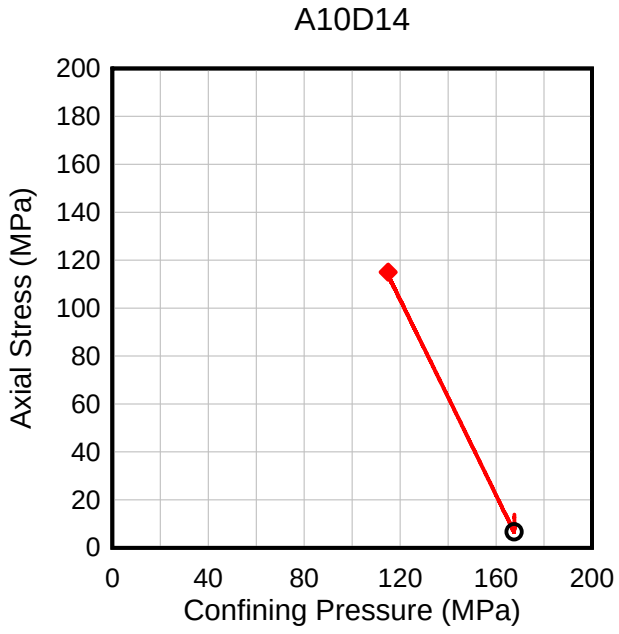

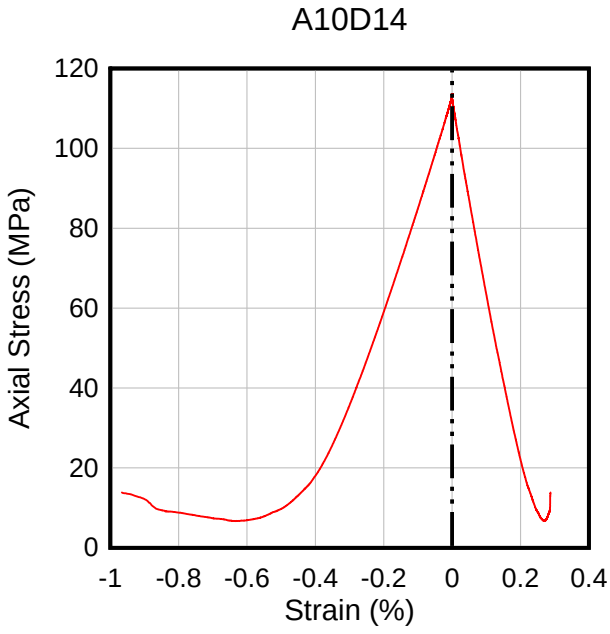

Test F18A/B – Triaxial Extension at 150 MPa Mean Stress

Pre-test

Post-test

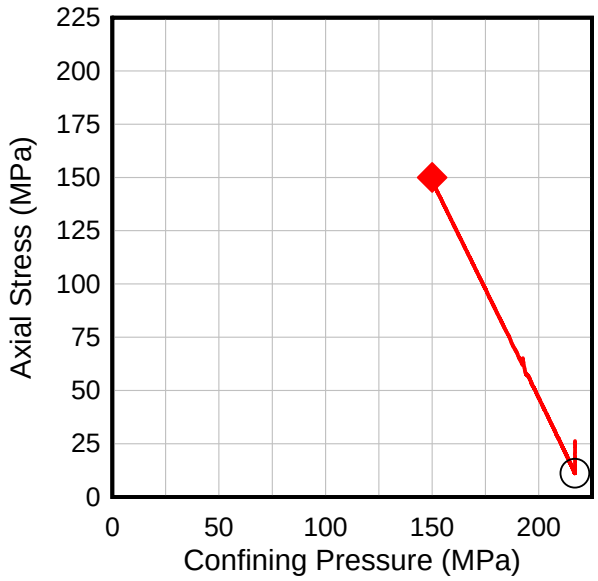

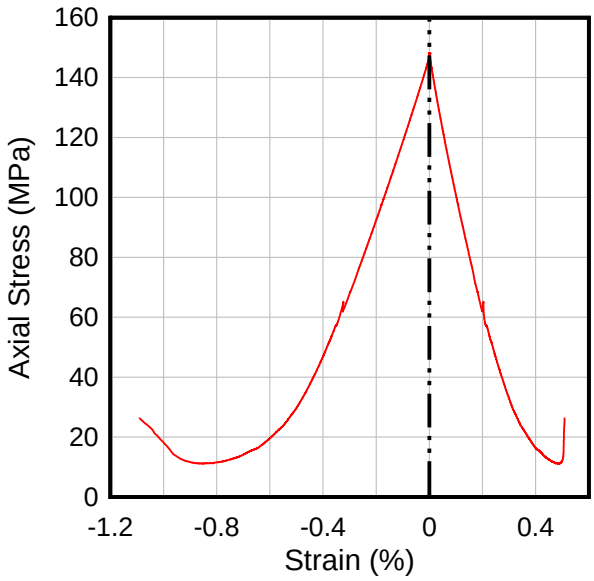

Test F11A/B – Triaxial Extension at 200 MPa Mean Stress

Pre-test

Post-test

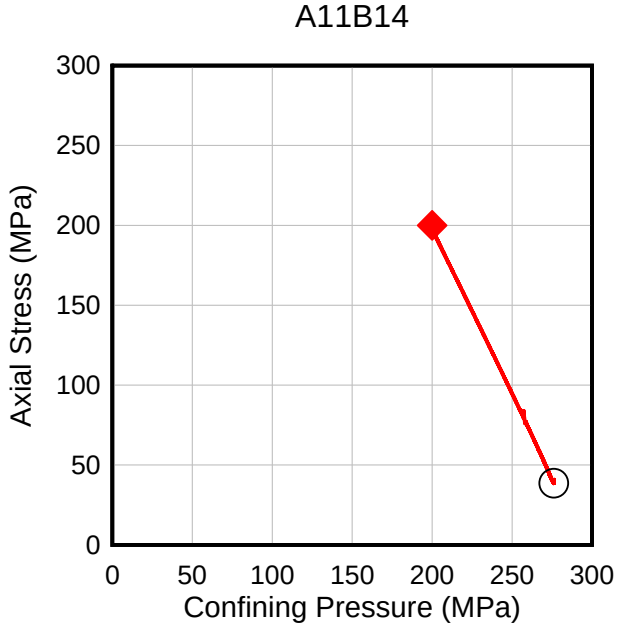

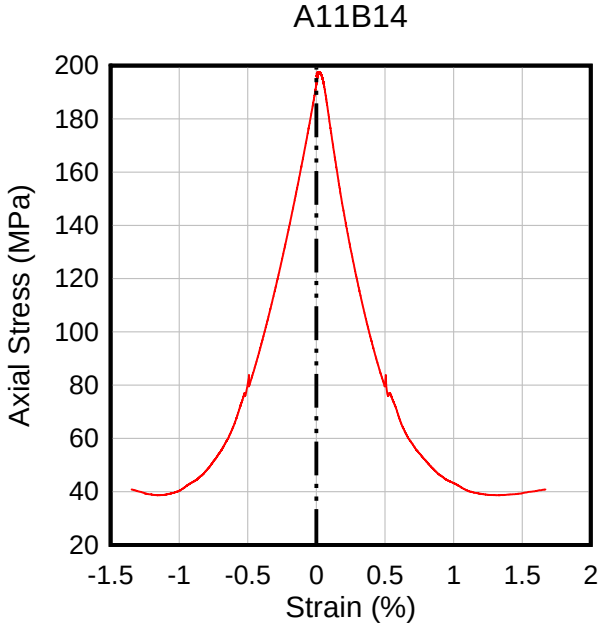

Test F13A/B – Triaxial Extension at 250 MPa Mean Stress

Pre-test

Post-test

F13B13

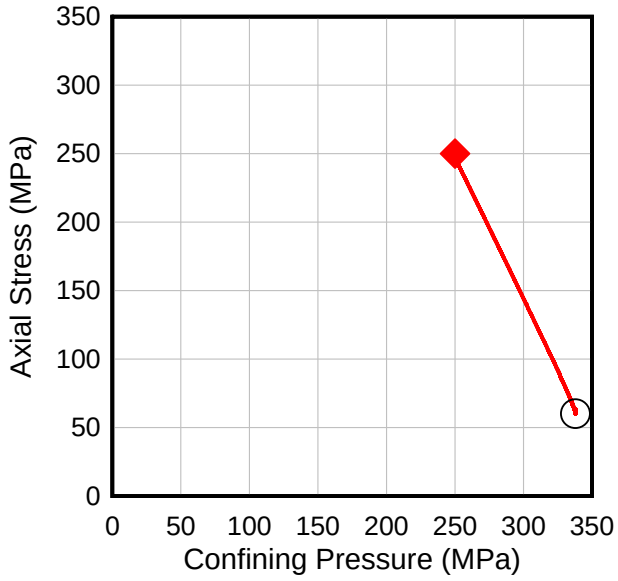

F13B14

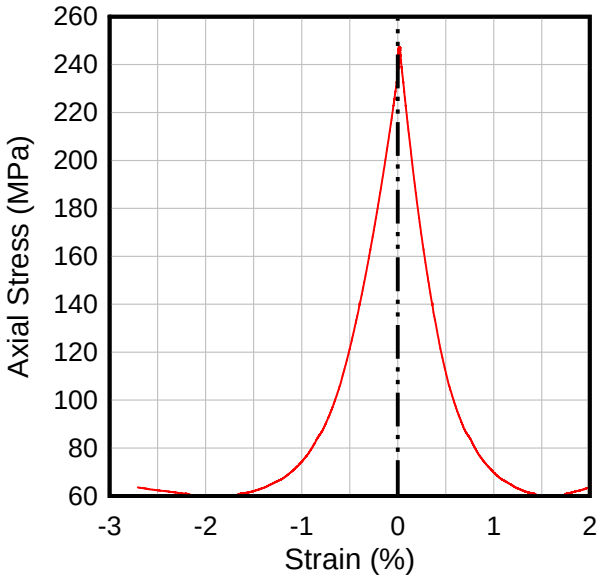

8. Appendix B – Confined Tension (CT) Data and Photos

Test M4A14 – Confined Tension at 0.0 MPa (Unconfined)

Pre-test

Post-test

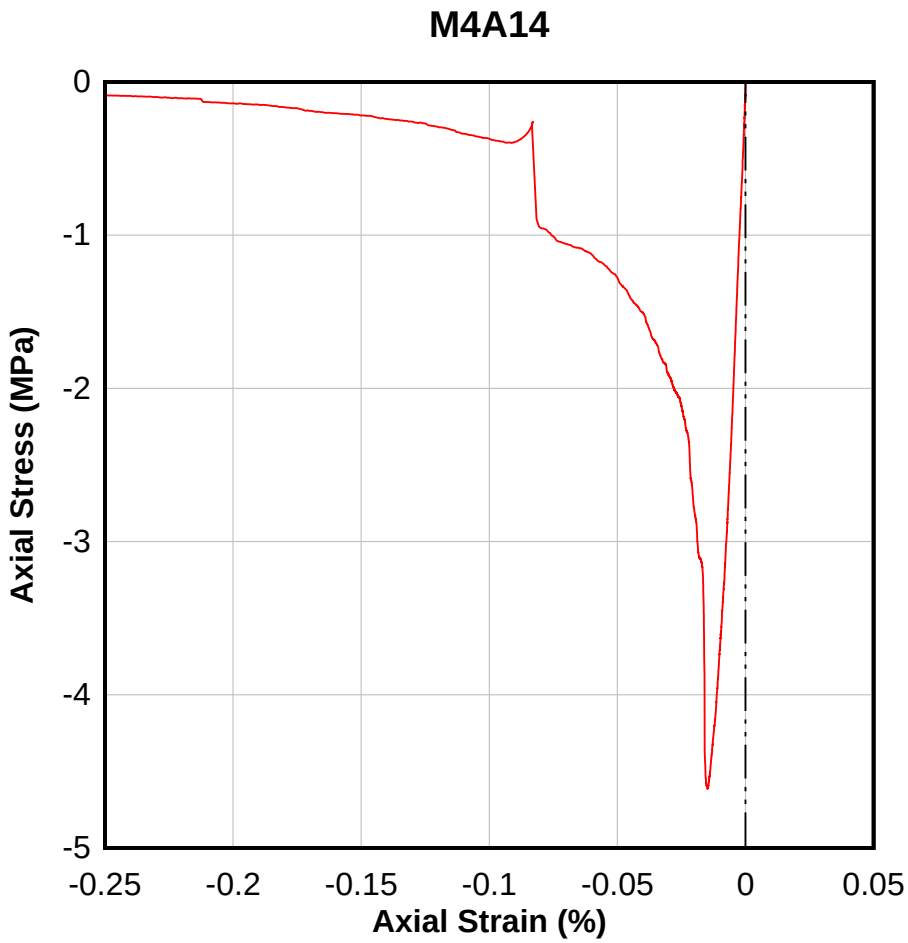

Test M5A/B14 – Confined Tension at 22.3 MPa

Pre-test

Post-test

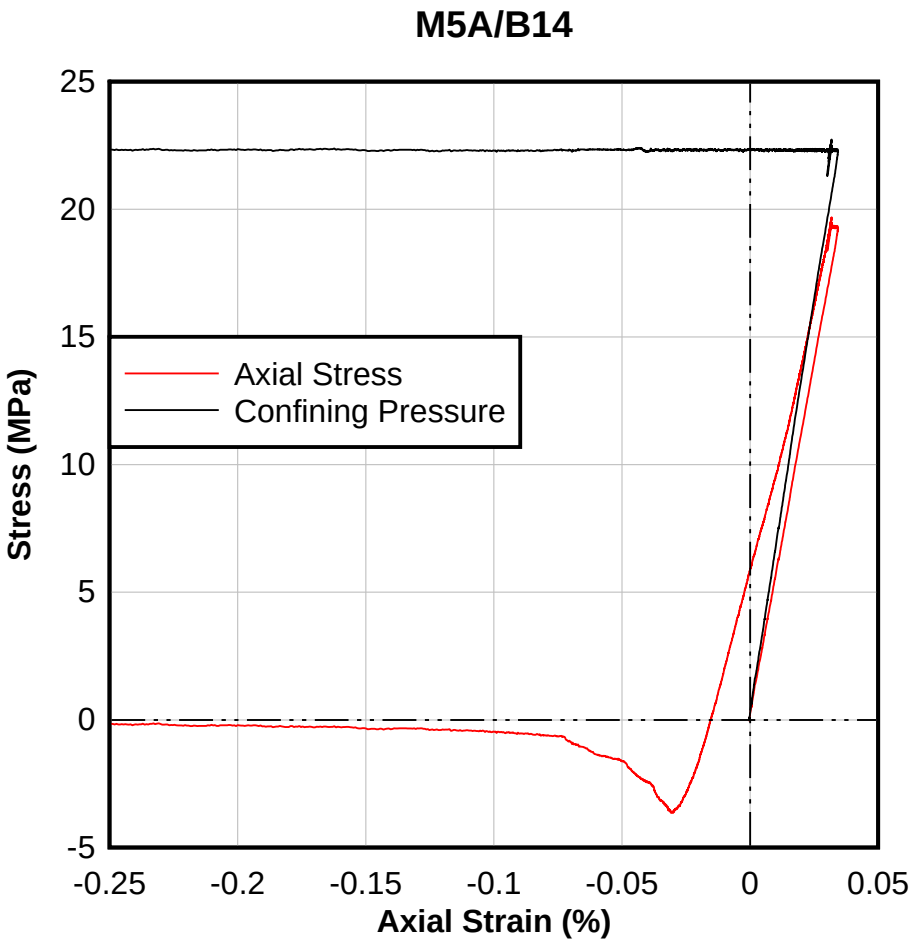

Test A9A/B14 – Confined Tension at 35.0 MPa

Pre-test

Post-test

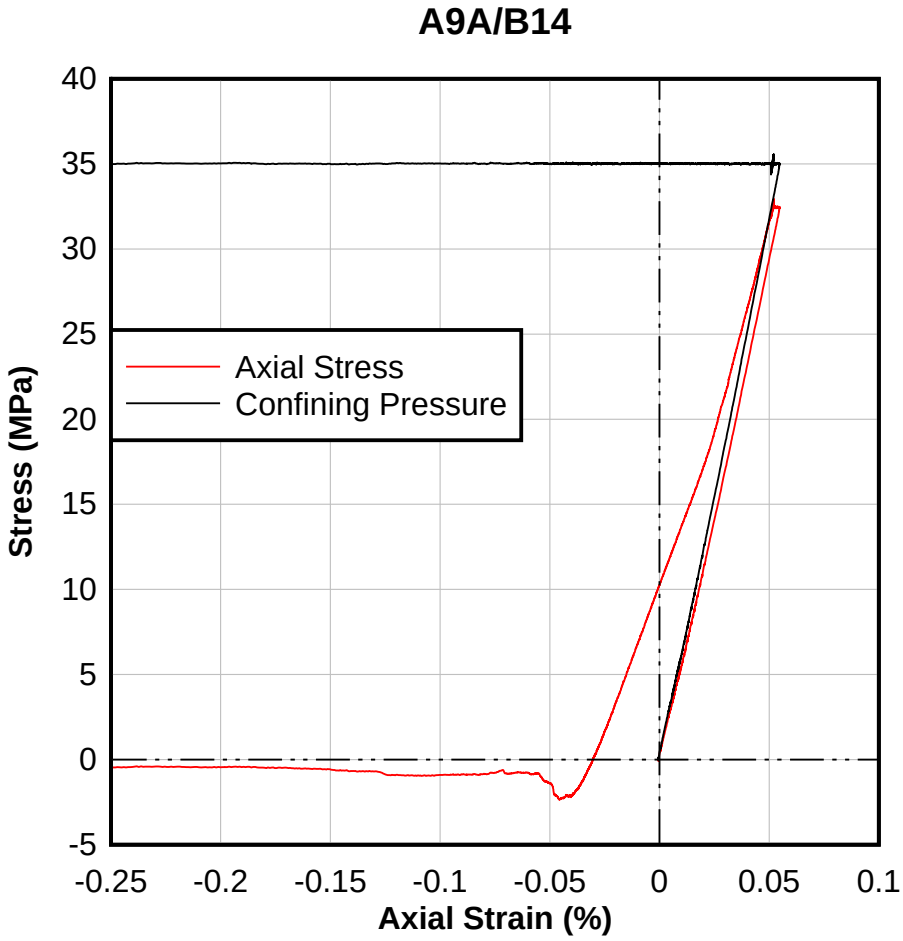

Test M6A/B14 – Confined Tension at 44.6 MPa

Pre-test

Post-test

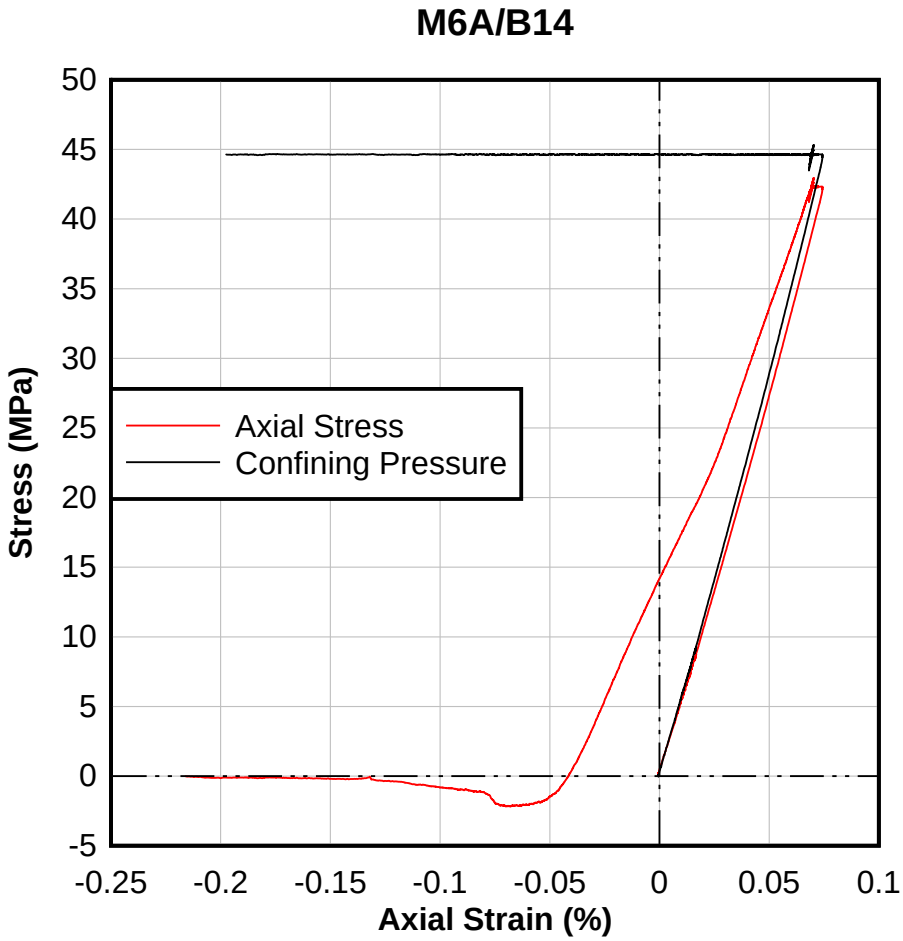

Test A9C/D14 – Confined Tension at 65.0 MPa

Pre-test

Post-test

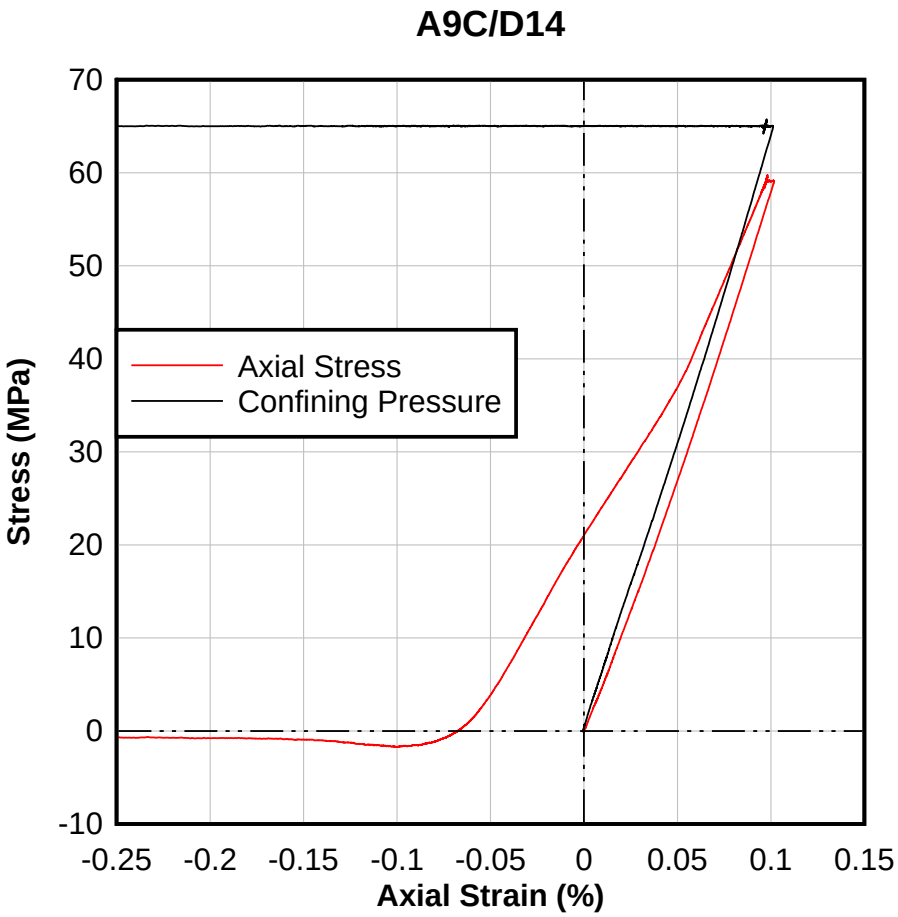

DISTRIBUTION LIST
AFRL-RW-EG-TR-2014-120

Defense Technical Information Center Attn: Acquisition (OCA) 8725 John J. Kingman Road, Ste 0944 Ft Belvoir, VA 22060-6218	1 Electronic Copy (1 File & 1 Format)

EGLIN AFB OFFICES:

AFRL/RWOC (STINFO Office)	1
AFRL/RW CA-N	STINFO Officer Provides Notice of Publication
AFRL/RWMW (Attn: Matt Matyac)	1
AFRL/RWP (Attn: Howard White)	1
AFRL/RWML (Attn: Mark Green)	1
AFRL/RWML (Attn: Martin Schmidt)	1
AFRL/RWML (Attn: Brian Plunkett)	1

1 copy each to:

Lawrence Livermore National Laboratory
Attn: Tarabay Antoun
M/S L-286
P.O.Box 808
Livermore, CA 94551-0808

Lawrence Livermore National Laboratory
Attn: Tony DePiero
M/S L-125
7000 East Avenue
Livermore, CA 94551-0808

Lawrence Livermore National Laboratory
Attn: Dan Badders
M/S L-125
7000 East Avenue
Livermore, CA 94551-0808

Sandia National Laboratories
Attn: Doug Dederman/Eric Klamerus
1515 Eubank Blvd. SE
M/S 1160
Albuquerque, NM 87123

Lawrence Livermore National Laboratory
Attn: Doug Stillman
M/S L-125
7000 East Avenue
Livermore, CA 94551-0808